03,07,13

On the brittleness of elementary semiconductors

© M.N. Magomedov

Institute for geothermal problems and renewable energy —
branch of the joint Institute of high temperatures of the Russian Academy of Sciences,
Makhachkala, Russia

E-mail: mahmag4@mail.ru

Received November 7, 2022
Revised November 15, 2022
Accepted November 18, 2022

It is shown that the brittleness of a single-component covalent crystal (diamond, Si, Ge) is due to the „duplicity" of the paired potential of interatomic interaction for elastic (reversible) and for plastic (irreversible) deformation. This leads to the fact that the specific surface energy during plastic deformation of a covalent crystal is more than two times less than the specific surface energy during elastic deformation. Therefore, with a small deformation of a covalent crystal, it is energetically more advantageous to create a surface by irreversible breaking than by reversible elastic stretching. It is indicated that the brittle-ductile transition in a single-component covalent crystal is accompanied by metallization of covalent bonds on the surface. It is shown that the brittle-ductile transition temperature (T_{BDT}) for single-component covalent crystals under static load has an upper limit: $T_{BDT}/T_m < 0.45$, where T_m — is the melting temperature.

Keywords: interatomic covalent bond, brittleness, ductility, elementary semiconductors, brittle-ductile transition.

DOI: 10.21883/PSS.2023.02.55401.521

1. Introduction

Brittleness is defined as the property of a material that fractures without visible permanent strain. For brittle materials, elongation at break is not higher than 2−5%, and in some cases it is equal to decimal places of one percent. Elemental semiconductors: diamond (C-dia), silicon (Si), germanium (Ge) feature brittleness due to covalent type of bond [1–5]. They have different brittle-ductile transition temperature (T_{BDT}), but brittleness remains up to the temperatures that are much higher than metal melting temperature (T_m) [4]. In this case, the brittle-ductile transition temperature grows with the decrease in metallic bond share.

$$T_{BDT}(\text{C-dia}) > T_{BDT}(\text{Si}) > T_{BDT}(\text{Ge}).$$

At temperatures higher than T_{BDT}, the material undergoes ductile fracture, below T_{BDT} the material undergoes brittle fracture. Depending on any defects and impurities, strain rate and specimen illumination, T_{BDT} in elemental semiconductors may vary in a wide temperature range [1–6]. For example, for Si, the following was determined [6]:

$$0.32 \leq \frac{T_{BDT}}{T_m} \leq 0.7.$$

The origin of brittleness of elemental semiconductors is still unexplained [5–10]. Moreover, it is not clear why the fracture is formed without any visible plastic flow under bending of these crystals at $T < T_{BDT}$? The existing brittle fracture theories are based on the classical theory of reversible small-strain elasticity [7–10]. When these theories address fracture propagation in a substance, they generally do not address the fracture initiation issue. The existing theories do not consider that elastic deformation is a reversible process and fracture initiation is an irreversible process. Moreover, a facture is generally initiated on the surface rather than within a deformed body. Brittle-ductile properties of a substance are governed by the surface conditions (Rehbinder effect) [11]. This is also indicated by the change in brittle-ductile properties of crystals when their surface is illuminated [8].

Earlier publications suggested that transition from brittle to ductile fracture of crystal was due to linear defects — dislocations — occurring during deformation [2–4]. However, dislocations, like other less energy-consuming defects (vacancies, interstitial atoms, etc.) propagate within the crystal structure. They accompany the growth of the existing fracture, shield it and influence on the fracture propagation rate. But the dislocation model still could not explain the fracture initiation on a crystal surface and could not offer any brittle-ductile transition temperature calculation method in single-component covalent crystals [7–10]. In addition, the dislocation model cannot explain glass or ceramics brittleness because a dislocation (either edge or screw dislocation) is a linear defect in a crystal structure.

Therefore, a new approach to this problem is offered herein. Based on the pair covalent bond model offered in [12], this publication explains reasons of fracture initiation on a semiconductor crystal surface at $T < T_{BDT}$ and transition to ductile state at $T > T_{BDT}$. In addition, no assumption on dramatic generation of dislocations (or other defects) at brittle-ductile transition temperature will not be used herein.

2. Pair interatomic covalent bond energy

We present a pair interatomic interaction in a single-component crystal in the form of the Mie–Lennard-Jones potential as follows:

$$\varphi(r) = \frac{D}{(b-a)}\left[a\left(\frac{r_0}{r}\right)^b - b\left(\frac{r_0}{r}\right)^a\right], \qquad (1)$$

where D and r_0 are the depth and coordinate of the potential minimum and $b > a > 1$ are numerical parameters.

Since for carbon subgroup elements, „zero point" energy of atoms is two to three orders lower than the interatomic bond energy, then the following expressions may be used with good accuracy in order to determine r_0, b and a [12,13]:

$$r_0 = \left(\frac{6k_pV_{00}}{\pi N_A}\right)^{1/3}, \quad b = 6\gamma_{00} - 2,$$

$$a = 3\left[B'(P)_{00} - 2\right] - b. \qquad (2)$$

Here, V is the molar volume, N_A is the Avogadro number, k_p is the structure packing factor, $\gamma = -[\partial \ln(\Theta)/\partial \ln(V)]_T$ is the Grüneisen parameter, Θ is the Debye temperature, $B = -V(\partial P/\partial V)_T$ is the isothermal modulus of elasticity, $B'(P) = (\partial B/\partial P)_T$ is the derivative of the modulus of elasticity by pressure. Index „00" means that this value was defined at zero temperatures and pressures, i.e. at $T = 0\,\mathrm{K}$ and $P = 0$.

The depth of the potential well can be determined by two ways: from the modulus of elasticity B_{00} and from the atomization energy (per atom) L_{00} at $T = 0\,\mathrm{K}$ and $P = 0$ [12,13]:

$$D_b = \frac{18B_{00}V_{00}}{k_n a b N_A} = D_s + \Delta D, \quad D_s = \frac{L_{00}}{k_n/2}, \qquad (3)$$

where k_n is the first coordination number, $\Delta D = D_b - D_s$ is the variation in results.

For metals, D_b and D_s are usually the same, i.e. $\Delta D = 0$. However, for covalent crystals $D_b \gg D_s$ as shown in Table 1. And in transition from diamond to Si, Ge and α-Sn, ΔD is gradually decreasing with the increase in atom weight (m), and becomes close to zero for lead: $\Delta D(\mathrm{Pb}) \approx 0$ (see Table 1). For C-dia, Si, Ge and α-Sn, the following condition is met: $\Delta D = (D_b/2) + d \approx D_b/2$. Therefore, the pair interatomic bond in a covalent crystal may be presented in a form of two bonds, where each

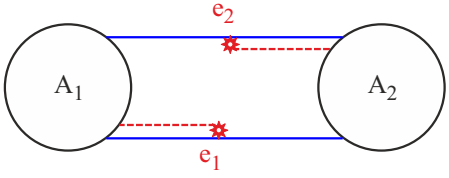

Figure 1. Diagram of pair interatomic bond in a covalent crystal.

Table 1. Interatomic potential parameters (1) calculated using expressions (2) and (3), and ΔD and $d = \Delta D - (D_b/2)$ calculated on their basis

Element m, a.m.u.	r_0, Å	b	a	D_b, eV	D_s, eV	ΔD, eV	d, eV	$\Delta D/D$
C-dia 12.01	1.545	3.79	2.21	8.43	3.68	4.75	0.535	1.291
Si 28.09	2.351	4.00	2.48	5.54	2.32	3.22	0.450	1.388
Ge 72.59	2.450	4.30	2.75	4.03	1.94	2.09	0.075	1.077
α-Sn 118.7	2.798	4.43	2.79	3.15	1.56	1.59	0.015	1.019
Pb 207.2	3.500	14.2	2.38	0.378	0.338	0.04	−0.149	0.118

of them is formed by a valence electron in each of the interacting atoms [12]. Two shared electrons in the covalent bond make two bonds each: with „own" ion (strong bond) and with „alien" ion (weak bond). According to this, covalent bond between the pair of atoms may be presented in the form of two links which are shown schematically in Figure 1.

Figure 1 shows a symmetrical double interatomic bond (consisting of two asymmetrical single bonds) formed by two shared valence electrons. The total pair interatomic bond energy is equal to: $D_b = D_s + \Delta D = D_s + (D_b/2) + d = 2(D_s + d)$. The single bond energy is: $D_b/2 = D_s + d$. Here, $D_s/2 = L_{00}/k_n$ is the weak single bond energy, i.e. the bond energy of a shared electron in a covalent bond with „alien" ion. This bond is schematically shown by a solid line: $\mathrm{A}_1 - \mathrm{e}_2$ or $\mathrm{A}_2 - \mathrm{e}_1$. $\Delta D/2 = (D_s/2) + d$ is the strong single bond energy, i.e. this is the energy of bond between the electron and its „own" ion. This bond is shown by a double (solid and dashed) line: $\mathrm{A}_1 = \mathrm{e}_1$ or $\mathrm{A}_2 = \mathrm{e}_2$, where the solid line shows $D_s/2$, and the dashed line shows the difference between the strong and weak bond energies, i.e. this is a difference between the bond energies of the electron and its „own" ion and the electron and the „alien" ion: $d = \Delta D - (D_b/2) - D_s = (\Delta D - D_s)/2$. The single bond energy provided by each shared valence electron is equal to: $D_b/2 = (L_{00}/k_n) + (\Delta D/2) = D_s + d$. In case of metallic covalent bonding, links connecting the electrons with their „own" ions (double lines $\mathrm{A}_1 = \mathrm{e}_1$ and $\mathrm{A}_2 = \mathrm{e}_2$ whose energy is $\Delta D = D_s + 2d$) are broken and only one metallic bond remains, i.e. one solid line $\mathrm{A}_1 - \mathrm{A}_2$ whose energy is D_s.

As we have shown before in [14–18], in case of elastic (reversible) deformation of a covalent crystal, strong and weak covalent bond links are involved simultaneously and the potential depth (1) is equal to D_b. This is D_b that shall be used for calculation of such parameters which are

measured without breaking interatomic bonds: speed of sound, Debye temperature, thermal expansion coefficient. In case of plastic (irreversible) deformation of a covalent crystal, only weak bond links are broken and the potential depth (1) is defined by D_s. Therefore, D_s defines the parameters (associated with interatomic bond breakage) such as sublimation energy $L_{00,}$ specific surface energy, vacancy formation and self-diffusion energy. As shown in [15] for Si or Ge semiconductor phase, the equation of state is described on the basis of elastic-type interatomic potential, and for pressure-bonded Si or Ge phases — the equation of state is described on the basis of plastic-type interatomic potential. Due to this „duplicity" of the pair interatomic potential for a covalent crystal, no single interatomic potential has been offered so far on the basis of more complex (than (1)) functionalities that include a greater number of fitting parameters than potential (1) [5,16].

3. Fracture initiation condition

When a new surface is formed under infinitely low bending of a covalent crystal, then this infinitely low increase in the surface area δS may be achieved by two methods.

1. By reversible elastic surface tension. Then the specific (per unit area) surface energy σ_b will be derived from the elastic-type potential, i.e. from D_b.

2. By irreversible brittle surface fracture. Then σ_s will be derived from the plastic-type potential, i.e. from D_s.

For a covalent crystal, the following energy shall be input in the first case: $E_b = \sigma_b \delta S$, and in the second case: $E_s = \sigma_s \delta S$. Therefore, the following inequality is a prerequisite for brittle fracture

$$\Delta E = E_b - E_s = (\sigma_b - \sigma_s)\delta S \geq 0. \tag{4}$$

Condition (4) means that formation of a surface by means of brittle fracture is more beneficial in term of energy than by means of elastic deformation. Condition (4) also indicates the presence of two energy levels in the system, i.e. the system is also able to form a surface by means of fracture, in addition to elastic deformation. For an equilibrium metallic single crystal, i.e. a crystal without metastable stress or nanostructured areas, $\Delta E = 0$ is met.

The following inequality is a prerequisite for brittle fracture

$$\Delta E = (\sigma_b - \sigma_s)\delta S \geq \sigma_s \delta S. \tag{5}$$

Condition (5) means that the advantage in energy under brittle fracture is higher than the energy required for formation of a new surface. It is evident that the higher $\Delta E/(\sigma_s \delta S) = (\sigma_b - \sigma_s)/\sigma_s$, the higher the probability of brittle fracture of a covalent crystal under deformation is.

Thus, according to (5), the brittle-ductile transition temperature may be calculated as follows

$$\sigma_b(T_{BDT}) = 2\sigma_s(T_{BDT}). \tag{6}$$

Using the interatomic potential (1) and the „only nearest neighbors interaction" approximation and using the Einstein model for crystal vibration spectrum, the following expression was obtained for the specific face surface energy (100) of a crystal [17–19]:

$$\sigma(100) = -\frac{k_n D R^2}{12\alpha^{2/3} r_0^2}\left[U(R) + \frac{18\gamma}{b+2}\frac{k_B \Theta_E}{D k_n} E_w\left(\frac{\Theta_E}{T}\right)\right]. \tag{7}$$

Here, k_B is the Boltzmann constant, $R = r_0/c$ is the linear density, $c = (6k_p\nu/\pi)^{1/3}$ is the distance between centers of the nearest atoms, $\nu = V/N$ is the specific volume (per atom), $\alpha = \pi/(6k_p)$, Θ_E is the Einstein temperature associated with the Debye temperature as follows [13]: $\Theta = (4/3)\Theta_E$, other functions are as follows

$$U(R) = \frac{aR^b - bR^a}{b-a}, \quad E_w(y) = 0.5 + \frac{1}{[\exp(y) - 1]},$$
$$y = \frac{\Theta_E}{T} = \frac{3\Theta}{4T}. \tag{8}$$

Using the interatomic potential (1) and the „only nearest neighbors interaction" approximation, the Debye temperature can be calculated as [20]:

$$\Theta(k_n, c) = A_w(k_n, c)\xi\left[-1 + \left(1 + \frac{8D}{k_B A_w(k_n, c)\xi^2}\right)^{1/2}\right], \tag{9}$$

where function A_w takes into account „zero ascillations" of crystal atoms

$$A_w(k_n, c) = K_R \frac{5k_n a b(b+1)}{144(b-a)}\left(\frac{r_0}{c}\right)^{b+2},$$
$$K_R = \frac{\hbar^2}{k_B r_0^2 m}, \quad \xi = \frac{9}{k_n}. \tag{10}$$

Here: m is the atomic mass, $\hbar$ is the Planck's constant.

From equation (9), the Grüneisen parameter is expressed as:

$$\gamma = -\left(\frac{\partial \ln \Theta}{\partial \ln \nu}\right)_T = \frac{b+2}{6(1+X_w)}, \tag{11}$$

where function $X_w = A_W \xi/\Theta$ is introduced to define the role of quantum effects.

Equations (7), (9) and (11) were tested for many substances at various temperatures and pressures and agreed well with the specific surface energy [14,17–19], Debye temperature and Grüneisen parameter [20] measurements. Therefore we used these equations to calculate functions $\sigma_b(T)$ and $\sigma_s(T)$.

4. Brittle-ductile transition temperature

According to [14,17–19], actual specific surface energy for a crystal with covalent bond shall be derived from D_s. σ_s values calculated in this way meet the measured and calculated (in brackets) specific surface energies shown for

Table 2. Specific surface energies of the face (100) at $T = 0\,\mathrm{K}$ and $P = 0$ calculated using (7)–(11). (σ_b was calculated from D_b and σ_s was calculated from D_s. Lower lines show the experimental and theoretical (in brackets) specific surface energies of the face (100) from [21-26])

Crystal	σ_b, $10^{-3}\,\mathrm{J/m^2}$	σ_s, $10^{-3}\,\mathrm{J/m^2}$	$\sigma_b - \sigma_s$, $10^{-3}\,\mathrm{J/m^2}$	$(\sigma_b - \sigma_s)/\sigma_s$
C-dia [17]	14025.0	6104.5	7920.50	1.297
Experiment and (theory)	$(9720_{\mathrm{ideal}} - 5710_{\mathrm{recons}})^{1)}$ [23], $(6231.9_{\mathrm{ideal}} - 4969.1_{\mathrm{recons}})^{1)}$ [24], (4458) [26]			
Si [18]	4001.10	1673.42	2327.68	1.391
Experiment and (theory)	2130 [21], 1360 [22], $(2390_{\mathrm{ideal}} - 1410_{\mathrm{recons}})^{1)}$ [23], $(1879.8_{\mathrm{ideal}} - 1010.9_{\mathrm{recons}})^{1)}$ [24], (1280) [25], (1314) [26]			
Ge [19]	2681.50	1290.32	1391.18	1.078
Experiment and (theory)	1835 [21], $(1710_{\mathrm{ideal}} - 1000_{\mathrm{recons}})^{1)}$ [23], $(1657.2_{\mathrm{ideal}} - 883.1_{\mathrm{recons}})^{1)}$ [24], (870) [25], (1002) [26]			

Note. [1)] Design surface energies of ideal (nonrelaxed) and reconstructed (relaxed) surfaces (100).

each crystal in the lower lines in Table 2. As shown in Table 2, „elastic“ specific surface energy $\sigma_b(T = 0\,\mathrm{K})$ derived from D_b is much higher than the measured value.

During isobaric temperature growth as a result of thermal covalent bonding, function $\sigma_b(T)$ is reduced. Therefore, it can be calculated using the following expression:

$$\sigma_b(T) = \sigma_b(0)\left[1 - \exp\left(-\frac{H_s}{k_B T}\right)\right], \qquad (12)$$

where H_s is the energy required for covalent bonding on the crystal surface.

At the melting temperature (T_m) due to full covalent bonding within the crystal structure, function $\sigma_b(T)$ must satisfy the following condition

$$\sigma_b(T_m) = \sigma_s(T_m). \qquad (13)$$

From (12) and (13), he following expressions may be derived

$$H_s = -k_B T_m \ln\left[1 - \frac{\sigma_s(T_m)}{\sigma_b(0)}\right],$$

$$\sigma_b(T) = \sigma_b(0)\left\{1 - \left[1 - \frac{\sigma_s(T_m)}{\sigma_b(0)}\right]^{T_m/T}\right\}. \qquad (14)$$

Since at T_{BDT}, condition (6) is met, then the following equation can be easily derived from (14)

$$\frac{T_{BDT}}{T_m} = \ln\left[1 - \frac{\sigma_s(T_m)}{\sigma_b(0)}\right] \Big/ \ln\left[1 - \frac{2\sigma_s(T_{BDT})}{\sigma_b(0)}\right] = \frac{\ln(1-x)}{\ln(1-2x+\Delta)}. \qquad (15)$$

The following notations are introduced here

$$x = \frac{\sigma_s(T_m)}{\sigma_b(0)} < 1, \quad \Delta = \frac{2[\sigma_s(T_{BDT}) - \sigma_s(T_m)]}{\sigma_b(0)} \ll 1. \qquad (16)$$

Table 3 shows values T_{BDT} at $\Delta = 0$ calculated using equation (15). For calculations, measured melting temperatures at $P = 1\,\mathrm{atm}$ were taken from [27]. $\sigma_b(0)$ values were taken from Table 2. $\sigma_s(T_m)$ was determined using two approaches.

1. Calculation of $\sigma_s(T_m)_s$ for defect-free solid crystal using (7). This data is shown for each crystal in the first line in Table 3.

2. The use of a measured value for metallized liquid phase $\sigma(T_m)_l < \sigma_s(T_m)_s$. This data from [28] for each crystal, are shown in the second lines in Table 3.

The data in Table 3 shows that good agreement with the measurements for T_{BDT} is achieved when measured $\sigma(T_m)_l$ for liquid phase was used in (15). This indicates that covalent bonds in solid phase of the specified crystals at T_m have not been metallized completely. In this case it should be taken into account that these calculations have been carried out for thermodynamic equilibrium state, i.e. without taking into account the deformation rate. According to the experiments [29], with growing deformation rate, the brittle-ductile transition temperature grows.

The following facts may be provided to prove that metallized of covalent bonding on the surface is the reason of brittle-ductile transition:

1. T_{BDT} for diamond meets the intensive surface graphitizing initiation temperature of diamond in vacuum: 1570–1600 K [1,30].

Table 3. Melting temperatures from [27], $\sigma_s(T_m)$ values calculated for solid phase (first line) and measured values for liquid phase (second line), T_{BDT} values calculated using equation (15) at $\Delta = 0$ and measured brittle-ductile transition temperatures from [1-4]

Crystal	T_m [27], K	$\sigma_s(T_m)$, 10^{-3} J/m^2	$\sigma_s(T_m)/\sigma_b(0)$	H_s, eV	T_{BDT}/T_m	T_{BDT}, K calculated	T_{BDT}, K experimental
C-dia	4235[1]	4975	0.355	0.160	0.354	1501	1470–1615 [1,4]
		~ 2805[2]	~ 0.2[2]	0.073	0.437	1850	
Si	1685	1565	0.391	0.072	0.325	548	820–1225 [2,4]
		746 [28][3]	0.186	0.029	0.442	745	
Ge	1210	1216	0.455	0.063	0.254	308	630–695 [3,4]
		605 [28][3]	0.226	0.027	0.426	516	

Note. [1)] Calculated value. [2)] Estimate for liquid phase. [3)] Measured value for liquid phase at $P = 1$ atm and T_m.

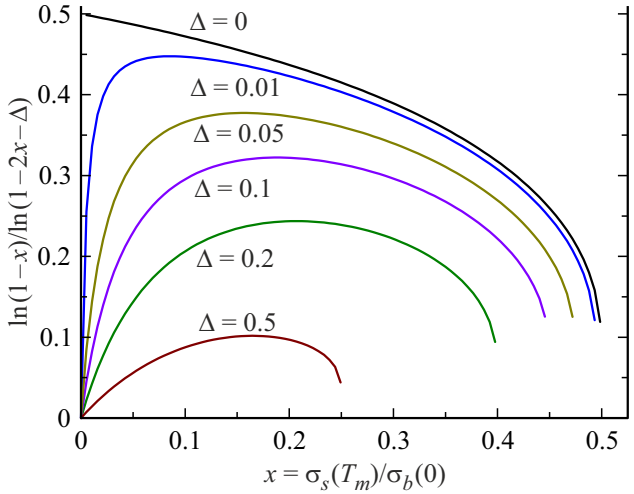

Figure 2. Variation of function (15) at different Δ values from (16).

2. Surface metallized of temperatures for Si(100) ($T > 900$ K [31]) and Ge(110) ($T > 750 \pm 50$ K [32]) are very close to measured T_{BDT} values for these crystals.

Tables 2 and 3 show that the following inequalities are met for argument x from (15) and (16):

$$0.186 < \frac{\sigma_s(T_m)_l}{\sigma_b(0)} < x = \frac{\sigma_s(T_m)_s}{\sigma_b(0)} < \frac{\sigma_s(0)}{\sigma_b(0)} < 0.482. \quad (17)$$

Figure 2 shows the dependence of function (15) vs. argument x at Δ from (16) from $\Delta = 0$ to $\Delta = 0.5$. Figure 2, (15) and (17) show that the following conditions are met for covalent crystals

$$\max\left[\frac{T_{BDT}}{T_m}\right] = 0.45, \quad \max\left[\frac{\sigma_s(T_{BDT})}{\sigma_b(0)}\right] = 0.5. \quad (18)$$

And it should be understood that these conditions have been derived from brittle-ductile transition under static load, i.e. at infinitely low deformation speed. With deformation rate growth, T_{BDT}/T_m increases [29].

It should be noted that brittleness of tempered or pressure-textured polycrystalline metals at low temperatures can also be explained by two possible interatomic potential values. For medium without intercrystalline boundaries (i.e. for an ideal equilibrium macrocrystal), use a „stable“ potential (1) with depth D_s, which may be determined from the atomization energy. For a metastable medium with strained polycrystalline structure, use a „metastable“ potential (1) with a depth D_b, which can be derived from the measured modulus of elasticity of this metastable structurally stressed medium. It is apparent that these potentials will give two different specific surface energies, for which conditions (6) and (13) may be used. But the values shown in (18) for an equilibrium covalent crystal, may be another for the metastable state.

For glass, this a metastable state of the substance, which may be also considered as a nanostructured single crystal [33].

5. Conclusion

A new analytical (without computer-based simulation) brittle-ductile transition temperature calculation method for single-component covalent crystals is offered.

It is shown that the covalent crystal brittleness is caused by „duplicity“ of a pair interatomic potential for elastic (reversible) and plastic (irreversible) deformation.

It is shown that the specific surface energy for a covalent crystal under plastic deformation is more than twice as low as the specific surface energy under elastic deformation. Therefore, at low deformation of a covalent crystal, it is more beneficial in terms of energy to form a surface by fracture than by elastic surface tension.

It is pointed out that the brittle-ductile transition in a single-component covalent crystal is followed by the metallization of paired covalent bonds on the surface.

It is shown that the brittle-ductile transition temperature for single-component covalent crystals under static load has an upper limit: $T_{BDT}/T_m < 0.45$.

Acknowledgments

The author would like to express hisgratitude to S.P. Kramynin, N.Sh. Gazanova, Z.M. Surkhayeva and M.M. Gadzhieva for fruitful discussions and assistance in work.

Conflict of interest

The author declares that he has no conflict of interest.

References

[1] V.I. Trefilov, Y.V. Milman, O.N. Grigoriev. Prog. Cryst. Growth Charact. **16**, 225 (1988). DOI: 10.1016/0146-3535(88)90019-6.
[2] P.B. Hirsch, S.G. Roberts. Phil. Mag. A **64**, *1*, 55 (1991). DOI: 10.1080/01418619108206126.
[3] F.C. Serbena, S.G. Roberts. Acta Metallurgica Mater. **42**, *7*, 2505 (1994). DOI: 10.1016/0956-7151(94)90331-x
[4] A. Giannattasio, S.G. Roberts. Phil. Mag. **87**, *17*, 2589 (2007). DOI: 10.1080/14786430701253197.
[5] A. Mattoni, M. Ippolito, L. Colombo. Phys. Rev. B **76**, *22*, 224103 (2007). DOI: 10.1103/PhysRevB.76.224103.
[6] G. Cheng, Y. Zhang, T.-H. Chang, Q. Liu, L. Chen, W.D. Lu, T. Zhu, Y. Zhu. Nano Lett. **19**, *8*, 5327 (2019). DOI: 10.1021/acs.nanolett.9b01789.
[7] T. Cheng, D. Fang, Y. Yang. J. Appl. Phys. **123**, *8*, 085902 (2018). DOI: 10.1063/1.5017171.
[8] H. Wang, S.I. Morozov, W.A. Goddard. Phys. Rev. B **99**, *16*, 161202 (2019). DOI: 10.1103/PhysRevB.99.161202.
[9] T. Zhang, F. Jiang, H. Huang, J. Lu, Y. Wu, Z. Jiang, X. Xu, Towards. Int. J. Extreme Manufact. **3**, *2*, 022001 (2021). DOI: 10.1088/2631-7990/abdfd7.
[10] G. Sun, X. Feng, X. Wu, S. Zhang, B. Wen. J. Mater. Sci. Technol. **114**, 215 (2022). DOI: 10.1016/j.jmst.2021.10.032.
[11] P.A. Rebinder, E.D. Shchukin. Sov. Phys. Usp. **15**, *5*, 533 (1973) DOI: 10.1070/PU1973v015n05ABEH005002
[12] M.N. Magomedov. Russ. J. Inorg. Chem. **49**, *12*, 1906 (2004).
[13] E.A. Moelwyn-Hughes. Physical Chemistry. Pergamon Press, London(1961). 1333 p.
[14] M.N. Magomedov. Tech. Phys. **58**, *12*, 1789 (2013). DOI: 10.1134/S1063784213120153.
[15] M.N. Magomedov. Phys. Solid State **59**, *6*, 1085 (2017). DOI: 10.1134/S1063783417060142.
[16] M.N. Esfahani. Solid State Commun. **344**, 114656 (2022). DOI: 10.1016/j.ssc.2022.114656.
[17] M.N. Magomedov. Tech. Phys. **62**, *5*, 661 (2017). DOI: 10.1134/S1063784217050176.
[18] M.N. Magomedov. Phys. Solid State **61**, *4*, 642 (2019). DOI: 10.1134/S106378341904019X
[19] M.N. Magomedov. Nanotechnol. Russ. **14**, *1–2* (2019) 21. DOI: 10.1134/S1995078019010063
[20] M.N. Magomedov. Tech. Phys. **58**, *9*, 1297. (2013). DOI: 10.1134/S106378421309020X
[21] R.J. Jaccodine. J. Electrochem. Soc. **110**, *6*, 524 (1963). DOI: 10.1149/1.2425806.
[22] D.J. Eaglesham, A.E. White, L.C. Feldman, N. Moriya, D.C. Jacobson. Phys. Rev. Lett. **70**, *11*, 1643 (1993). DOI: 10.1103/PhysRevLett.70.1643.
[23] A.A. Stekolnikov, F. Bechstedt. Phys. Rev. B **72**, *12*, 125326 (2005). DOI: 10.1103/PhysRevB.72.125326.
[24] J.M. Zhang, H.Y. Li, K.W. Xu, V. Ji. Appl. Surf. Sci. **254**, *13*, 4128 (2008). DOI: 10.1016/j.apsusc.2007.12.049.
[25] R. Tran, Z. Xu, B. Radhakrishnan, D. Winston, W. Sun, K.A. Persson, S.P. Ong. Sci. Data **3**, *1*, 1 (2016). DOI: 10.1038/sdata.2016.80.
[26] B. Fu. Adv. Mater. **8**, *2*, 61 (2019). DOI: 10.11648/j.am.20190802.14.
[27] R.R. Reeber. Mater. Res. Soc. Symp. Proc. Online Proc. Library (OPL) **453**, 239 (1996). DOI: 10.1557/PROC-453-239.
[28] B.B. Alchagirov, T.M. Taova, Kh.B. Khokonov. Transact. JWRI. Special Issue (Jpn) **30**, 287 (2001). https://repository.exst.jaxa.jp/dspace/handle/a-is/48071
[29] A.D. Evstifeev, A.A. Gruzdkov, Y.V. Petrov. Tech. Phys. **58**, *7*, 989 (2013). DOI: 10.1134/S1063784213070086.
[30] L. Chen, X. Yang, Q. Huang, C. Fang, A. Shi, R. Liu. Diamond Rel. Mater. **95**, 99 (2019). DOI: 10.1016/j.diamond.2019.04.003.
[31] L. Gavioli, M.G. Betti, C. Mariani. Phys. Rev. Lett. **77**, *18*, 3869 (1996). DOI: 10.1103/PhysRevLett.77.3869.
[32] A. Santoni, L. Petaccia, V.R. Dhanak, S. Modesti. Surf. Sci. **444**, *1–3*, 156 (2000). DOI: 10.1016/S0039-6028(99)01025-0.
[33] G.E. Abrosimova, D.V. Matveev, A.S. Aronin. Phys.–Usp. **65**, *3*, 227 (2022). DOI: 10.3367/UFNe.2021.04.038974

Translated by Ego Translating